

Efficiency of maximum entropy algorithm and GIS in assessing the landslide susceptibility

Mahdis Amiri¹  | Hamid Reza Asgari^{*2}  | Hamid Reza Pourghasemi³  |
Chooghi Bairam Komaki⁴ 

1. Dept. of Watershed and Arid Zone Management, Gorgan University of Agricultural Sciences and Natural Resources, Gorgan 4918943464, Iran. E-mail: mahdisamiri94@gmail.com
2. Corresponding Author, Dept. of Watershed and Arid Zone Management, Gorgan University of Agricultural Sciences and Natural Resources, Gorgan 4918943464, Iran. E-mail: hras2010@gmail.com
3. Dept. of Natural Resources and Environmental Engineering, College of Agriculture, Shiraz University, Shiraz, 71441-65186, Iran. E-mail: hamidreza.pourghasemi@gmail.com
4. Dept. of Watershed and Arid Zone Management, Gorgan University of Agricultural Sciences and Natural Resources, Gorgan 4918943464, Iran. E-mail: bkomaki@gmail.com

Article Info

Article type:
Research Full Paper

Article history:

Received: 07.06.2021
Revised: 12.17.2021
Accepted: 02.06.2022

Keywords:

AHP,
Effective factors,
Fars Province
Landslides susceptibility,
Maximum entropy,
ROC-AUC indicator,

ABSTRACT

Landslides is one of the most important natural disasters that cause excessive human and financial losses in mountain areas worldwide. There are appropriate methodologies for assessing risk and determining the effective risk factors associated with them. In this study, the maximum entropy by three replications was applied in Maxent software to investigate landslide susceptibility in the southern areas of Iran, Fars Province. To prepare the landslide susceptibility map, 13 factors were used: lithological units (Lu), land use/land cover (LULC), slope percentage (S_p), slope aspect (S_A), altitude, plan curvature (Plan-C), topographic wetness index (TWI), distance to river (DT_R), distance to roads (DT_{RS}), distance to fault (DT_F), drainage density (DD), normalized difference vegetation index (NDVI), and annual mean rainfall (AMR). After proving the lack of multicollinearity among the effective factors using tolerance (TOL) and variance inflation factor (VIF) indicators. On the other hand, the weighting of these 13 factors was determined using the AHP model. The results of the AHP method show that "Lithological units, Land use-cover and Slope percentage" are the most important influencing factor the occurrence of landslides in the study area. In real, three affecting factors ranked first to third in order of importance in the study area. Some of the landslide points were used for evaluate the built model according to the ROC/AUC indicator, in the other word, since 30% of the landslide points not used in modeling were randomly selected and used for evaluation. In addition, the final map of the landslide susceptibility by three replications had a good accuracy, whereas the third iteration with an AUC value of 0.778 (ROC=77.8%) had the highest accuracy in preparing the landslide susceptibility map. After that, the evaluation of landslide susceptibility maps with the second and third iterations with AUC values of 0.77 (ROC=77%) and 0.640 (ROC= 64%), respectively, had good and moderate accuracy with the highest efficiency in predicting landslide sensitivity. Finally, the highest percentage of landslide susceptibility area according to the first, second and third repetitions respectively in the moderate sensitivity class (0.03-0.1) with the value of 26.14%, the moderate sensitivity class (0.04-0.4). With a value of 25.91% and also in the moderate sensitivity class (0.04-0.1), there was the highest percentage of landslide area with a value of 25.71%. In general, landslides, due to their

dangerous nature in the highlands, suddenly disrupt the morphology and cause major damage to residential areas, roads, agricultural lands, etc. Therefore, landslides are a complex process that has a devastating effect on the environment and human life and requires investigation and preventive measures.

Cite this article: Amiri, Mahdis, Asgari, Hamid Reza, Pourghasemi, Hamid Reza, Komaki, Chooghi Bairam. 2022. Efficiency of maximum entropy algorithm and GIS in assessing the landslide susceptibility. *Journal of Water and Soil Conservation*, 28 (4), 53-76.



© The Author(s).

DOI: 10.22069/jwsc.2022.19292.3478

Publisher: Gorgan University of Agricultural Sciences and Natural Resources

Introduction

The inconsistency of natural slopes is a geomorphological and geological phenomenon that has an advantageous role in changing the shape of the Earth's surface and is very important because of the recurrence of this phenomenon and its harmful damage (Komac, 2006). The production of maps or forecasts of vulnerable areas on landslides is very important to prevent landslides and future plans for land use (Park, 2015). Landslide pattern analysis has played an important role in evaluating the structures and functions of various forms and forces in mountain ecosystems (Lopez et al., 2011). In the other hand, risk management and danger assessment of landslides begins with comprehensive identification and mapping, and this can be used to gain knowledge of spatial and temporal distribution (Brardinoni et al., 2003). In recent decades, owing to advances in computer sciences, geographic information systems (GIS) have been widely used to prepare and manage the affecting factors (e.g., slope, aspect, elevation, roads, rivers, etc.) on landslide susceptibility. Several studies have been conducted on landslide susceptibility assessment using remote sensing and GIS techniques (Pradhan et al., 2010; Regmi et al., 2014). Many qualitative and quantitative methods can be applied to landslide susceptibility evaluation (Faiz et al., 2018). Qualitative methods include inventory and knowledge-based methods. These mental methods are rarely used today. However, quantitative methods, which are based on physical data-based methods, are very effective in predicting landslide occurrence in spatial and temporal areas. These methods require precise geological engineering data, which are important for collecting large

areas (Schilirò et al., 2016). As a result, machine learning and soft computing methods have been widely applied to assess landslide sensitivity (Youssef et al., 2014; Elkadiri et al., 2014; Rahmati et al., 2019; Chen et al., 2019; Pandey et al., 2019). The Production of landslide maps describes past and current landslide occurrence, and mapping the spatial possibility of future landslide occurrence, landslide susceptibilities and risks are of great importance for land use planning, civil engineering works and decision making for landslide management (Broeckx et al., 2016; Bordoni et al., 2015; Pham et al., 2019), and GIS and RS integrated approaches used for the development of landslide susceptibility maps include the Frequency ratio (Shahabi et al., 2014; Wang et al., 2016). Discriminant Analysis, Analytic Hierarchy Processes (Pourghasemi and Rossi, 2016; Zhang et al., 2016), Logistic Regression (Shahabi et al., 2015; Tsangaratos et al., 2017), Bivariate Statistics (Youssef et al., 2015), Multivariate Regression (Conoscenti et al., 2015; Wang et al., 2015), Multivariate Adaptive Regression Splines (Felicísimo et al., 2013; Wang et al., 2015), Weights of Evidence (Kayastha et al., 2012; Tsangaratos et al., 2017), Weighted Linear Combinations (Akgun et al., 2008; Shahabi and Hashim, 2015), Evidential Belief Functions (Bui et al., 2015; Pourghasemi and Kerle, 2016) and Generalized Additive Models (Chen et al., 2017; Park and Chi, 2008). In addition to the above models, there are other methods such as artificial neural networks (Bui et al., 2016b; Dou et al., 2015), neuro-fuzzy (Nasiri Aghdam et al., 2016; Pradhan, 2013), boosted regression trees (Hong et al., 2015; Youssef et al., 2016), naïve Bayes (Pham et al., 2017; Shirzadi et al., 2017), decision trees (Pham et al., 2016; Tsangaratos and Ilia,

2016), and random forests (Chen et al., 2014; Hong et al., 2016) have also been applied for the development of landslide susceptibility maps.

The main objectives of the present study is to understand the characteristics of landslides, knowing the affecting factors, studying multi-collinearity between layers using TOL and VIF, accordingly selecting essential factors on landslides among the affecting factors on landslide susceptibility (Lu, LULC, S_p , S_A , Plan-C, TWI, DT_R , DT_{RS} , DT_F , DD, NDVI, and AMR) and prioritizing effective mentioned variables applying decision model such as "Analytic Hierarchy Processes" in the north of Fars province in Iran, also one of the most important innovations of this research is preparing landslide susceptibility map based on three repetitions (R1, R2 and R3) using maximum entropy in the Maxent software and finally selection the best repetition in the landslide map using AUC-ROC as a result, is chosen high

quality susceptibility map for landslide assessment in the study area. Choosing the best landslide assessment method helps managers and politicians identify landslide-sensitive areas based on similar conditions in the past, so they can take steps to prevent landslide sensitivity in sensitive areas.

Materials and Methods

Study area

The study area is located in southern Iran, Fars Province, at $30^{\circ} 3' 31''$ " to $30^{\circ} 32' 16''$ N and $51^{\circ} 21' 37''$ to $52^{\circ} 46' 14''$ " (Fig. 1). The area of Fars Province is approximately 122 thousand square kilometers which is 7.5% of the total area of Iran. The study region consists of four main watersheds, including the Karon Watershed, Dorodzan Dam Watershed, Zohreh Watershed, and Tashk-Bakhtegan Watershed in Fars Province.

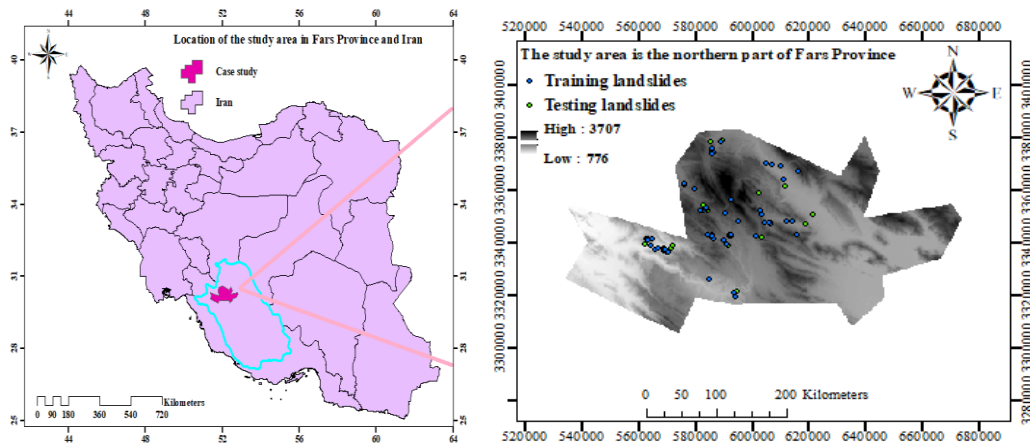


Fig. 1. The study area in Fars Province.

A flowchart of this study is shown in Fig. 2. The summary of the method and

material for this research includes the following steps:

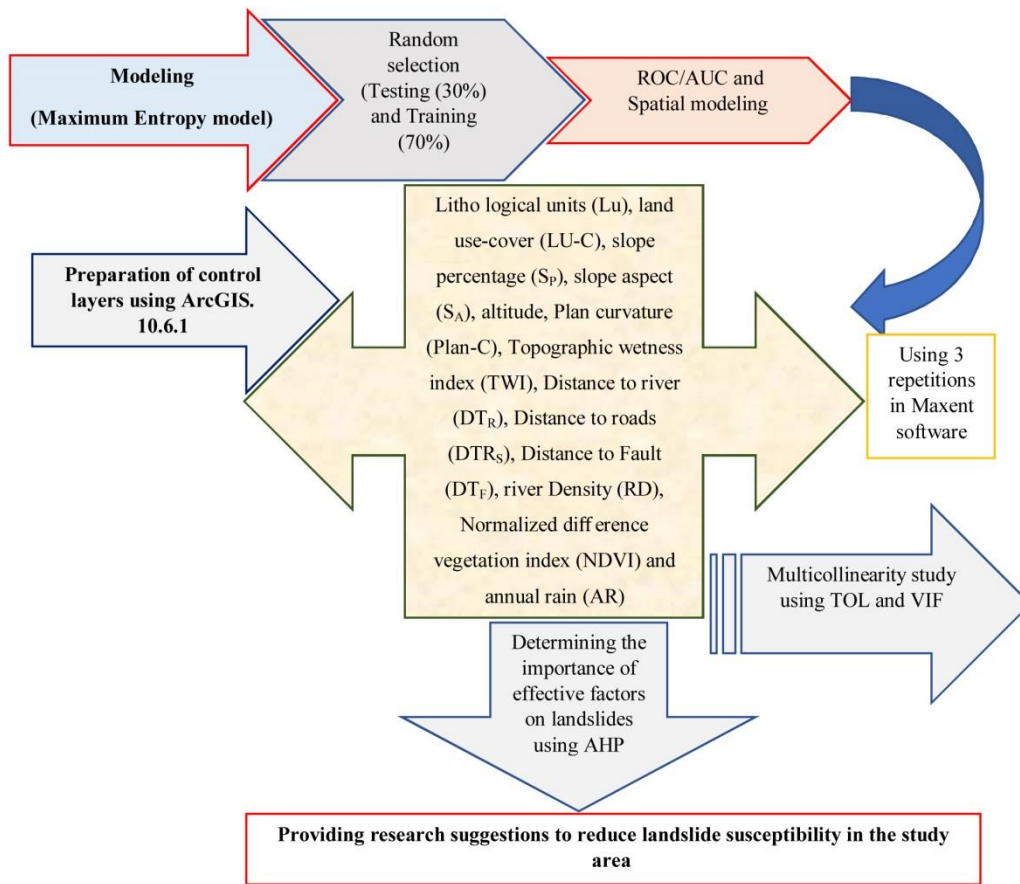


Fig. 2. The flowchart of the methodology practical in the study area.

Explanation of the landslide data

This study was based on a set of GIS-based data, which included the location of landslides and the factors influencing landslide occurrence mapping (LOM). Accordingly, a landslide distribution map was constructed through extensive field surveys and in total, 88 landslides were identified in the study area. The landslides were randomly divided into two groups data set including, modeling and validation (Kornejady et al., 2019; He et al., 2019). In the present study, the ratio between modeling and validation was selected 70:30, respectively. In addition, in our research, we created a landslide occurrence map according to three

replications in the Maxent software (Rahmati et al., 2019; Chen et al., 2019; Pandey et al., 2019), 13 landslide influencing factors, including (Lu), (LULC), (S_p), (S_A), altitude, (Plan-C), (TWI), (DT_R), (DT_{RS}), (DT_F), (DD), (NDVI), and (AMR) were selected and mapped in ArcGIS 10.6.1.

Altitude, Slope percentage (S_p), Slope aspect (S_A), Topographic wetness index (TWI), Plan curvature (Plan-C)

Because of the close connection of the landslide with the altitude (Meinhardt et al., 2015), a digital elevation model with a spatial resolution of 12.5 m was extracted from ALOS-DEM and used in this study (Fig. 3). The altitude variable specifies

the spatial distribution of landslides. In addition, altitude indirectly affects landslide occurrence through its important role in rainfall characteristics and vegetation type (He et al., 2019). Also, the probability of landslide occurrence is directly related to the slope angle (Nefeslioglu et al., 2008). The Slope percentage is indirectly related to the occurrence of landslides by affecting soil moisture and subsurface flow (Parker et al., 2016). The slope aspect has an important effect on wind and rain to be exposed to sunlight, so it shows the effective characteristics of the slope constituents (Galli et al., 2008). In general, the direction factor has an effect on other factors such as weathering, weather conditions, land, and soil cover, which is one of the important factors in landslide occurrence (He et al., 2019). In this study, the map of the slope aspect and slope angle were taken from the DEM (Fig. 3). TWI is another important factor in predicting landslide sensitivity and shows soil conditions and runoff volume (He et al., 2019). The TWI map was prepared from the DEM using the SAGA-GIS software (Fig. 3). Plan curvature describes the morphology of the topography. In particular, the slope curvature of the perpendicular line is the maximum of the slope in the direction of the domain, which makes it possible to highlight the convergence (concave curvature) and divergence (convex curvature) of the water flow (Trigila et al., 2015). In the other word, positive values represent convex, and negative values represent concavity. In this study, plan curvature was derived from a DEM with 12.5 a spatial resolution (Fig. 3).

Drainage density (DD), Distance to river (DT_R)

Drainage density is the ratio of the total length of waterways to the

watershed area. The higher the drainage density, the lower the permeability and the higher the surface flow rate (Yalcin, 2005). The drainage density map was extracted from the waterway lines and prepared using Spatial Analyst Tools in ArcGIS 10.6.1. In areas adjacent to rivers, due to the hydrological network, rapid soil saturation, and groundwater recharge, landslides are far greater than in areas farther away from rivers. There is a strong correlation between river distance and landslide susceptibility. This distance indirectly describes the erosion power of streams (Erener and Düzgün, 2010). The DT_R map was extracted from the waterway map and prepared using Spatial Analyst Tools and "Distance" in the Arc.GIS10.6.1 environment (Fig. 3).

Distance to roads (DT_{RS}), Distance to fault (DT_F)

Road construction is a human factor. Roads are generally built on slopes that limit the area behind the slope and develop cracks in the structure of the toes backing, such as faults (He et al., 2019). Therefore, distance to roads is one of the most important factors in the study of landslides (Liu et al., 2004). Fault surfaces easily occur on sliding surfaces because the stress on the rock surrounding a fault is unstable. Landslides repeatedly occur along surface ruptures (Yalcin et al., 2011). The distance to faults and road were determined from the fault map of the case study using "Distance Tools" in ArcGIS 10.6.1 (Fig. 3).

Lithological units (Lu)

The lithology of the area plays a very important role in assessing the sensitivity of landslides (Zhang et al., 2016). This is because lithology has a

significant effect on the hardship and weathering of rocks. Different lithological units have different effects on landslide outbreaks (Chen et al.,

2018). An explanation of the lithology units in the study area is presented in Table 1.

Table 1. Lithology of the study area.

Formation	Description	Lithological units	Age
-	Low level pediment fan and valley terrace deposits	Qft2, Qcf	Quaternary
Aghajari, Mishan	Brown to grey, calcareous, feature-forming sandstone and low weathering, gypsum- veined, red marl and siltstone	Mur, MuPlaj, Mmn, MPlfgp	Miocene
Bakhtyari	Alternating hard of consolidated, massive, feature forming conglomerate and low -weathering cross - bedded sandstone	Plc, Plbk	Pliocene
Jamal, Dorud	Massive to thick - bedded, dark - grey, partly reef type limestone and a thick yellow dolomite band in the upper part	Pj, P	Permian
-	Marl with intercalations of limestone	OMqm, OMql	Oligocene-Miocene
Taft	Thin to medium bedded argillaceous limestone and thick bedded to massive, grey orbitolina bearing limestone	Klsm, Klsol, Klsm, Ktl	Early Cretaceous
Jahrum	Grey and brown weathered, massive dolomite, low weathered thin to medium -bedded dolomite and massive, feature forming, buff dolomitic limestone	Eja, Ek	Eocene
Shemshak	Dark grey shale and sandstone	TRJs	Triassic-Jurassic
Lower Red	Red and green silty, gypsiferous marl, sandstone and gypsum	Olm,s,c	Oligocene
Shotori	Well - bedded, dense, yellow dolomite	TRsh	Early-Middle Triassic
Gurpi	Bluish grey marl and shale with subordinate thin - bedded argillaceous -limestone	Kgu	Cretaceous
Naiband	Sandstone, quartz arenite, shale and fossiliferous limestone	TRn	Mesozoic
-	Undivided Khami Group, consist of massive thin - bedded limestone comprising the following formations: Surmeh, Hith Anhydrite, Fahlian, Gadvan and Dariyan	JKkgp, KEpd-gu	Jurassic-Cretaceous
Khamehkat and Neyriz	Thin to medium - bedded, dark grey dolomite; thin - bedded dolomite, greenish shale and thin - bedded argillaceous limestone	TRe1, TRkknz	Triassic
Tarbur	Massive, shelly, cliff - forming partly anhydritic limestone	Ktb	Late Cretaceous
-	Undivided Asmari and Jahrum Formation, regardless to the disconformity separates them	EOas-ja	Paleocene-Oligocene
Baghamshah	Pale - green silty shale and sandstone	Jbg, Jf	Jurassic
Amphibolite Facies	Medium-grade, regional metamorphic rocks	pCmt1, pCmt2	Pre Cambrian

Continue Table 1.

Formation	Description	Lithological units	Age
Shidhtu	Alternation of shale, marl and fossiliferous limestone, locally with intercalations of quartz arenite	Dsh	Devonian
Pabdeh	Blue and purple shale and marl interbedded with the argillaceous limestone	PeEpd	Paleogene
Amiran	Dark olive - brown, low weathered siltstone and sandstone with local development of chert conglomerates and shelly limestone	KPeam	Cretaceous-Paleocene
-	Fluvial conglomerate, Piedmont conglomerate and sandstone	PIQc	Pliocene-Quaternary
-	Rock salt, gypsum & blocks of contorted masses of sedimentary material such as black laminated fetid limestone, brown cherty dolomite, red sandstone & varigated shale in association with igneous rocks such as diabase, basalt, rhyolite and trachyte	pC-Ch	Pre Cambrian-Cambrian
-	Granite	PZ2gr	Late Paleozoic
-	-	Lake	Late Eocene-Oligocene
Kerman and Neyzar Radiolarites	Purple and red thin - bedded radiolarian chert with intercalations of neritic and pelagic limestone	TRKurl, pd	Triassic-Cretaceous
Barreh Koshan Complex and Rutchan Complex	Gneiss, anatectic granite, amphibolite, kyanite, staurolite schist, quartzite and minor marble	Pz1mt	Early Paleocene
-	Gneiss and anatectic granite	Pz1gn	Early Paleozoic
Sachun	Pale red marl, marlstone, limestone, gypsum and dolomite	PeEsa	Paleocene-Eocene
Lalun	Dark red meddium - grained arkosic to subarkosic sandstone and micaceous siltstone	Cl	Cambrian
Sargaz Complex	Mica schist, green schist, graphite schist, black pyyllit and minor marble	DC2met	Devonian-Carboniferous
Surmeh	Thick - bedded to massive dolomitic limestone, thin - bedded argillaceous limestone and marl	Jsm	Early Middle Jurassic

Land use/ land cover (LULC)

Land use is of particular importance in slope instability and is highly related to landslide susceptibility (Zhao et al., 2015). In general, bare lands are more vulnerable to erosion than forested areas because the roots of the plants act as reinforcements and therefore prevent soil erosion (Beguiría, 2006). The land use map was taken from the Fars Natural Resources Department and updated using Google Earth (Fig. 3 and Table 2).

Normalized difference vegetation index (NDVI)

NDVI is a vital factor that is widely used to investigate the relationship between vegetation density and landslide susceptibility (Leventhal and Kotze, 2008). The Landsat 8 images (July and April, 2016) extracted from the USGS site (<https://earthexplorer.usgs.gov/>) and the NDVI map was prepared in ArcGIS10.6.1 environment (Eq. 1) (Pourghasemi et al., 2014).

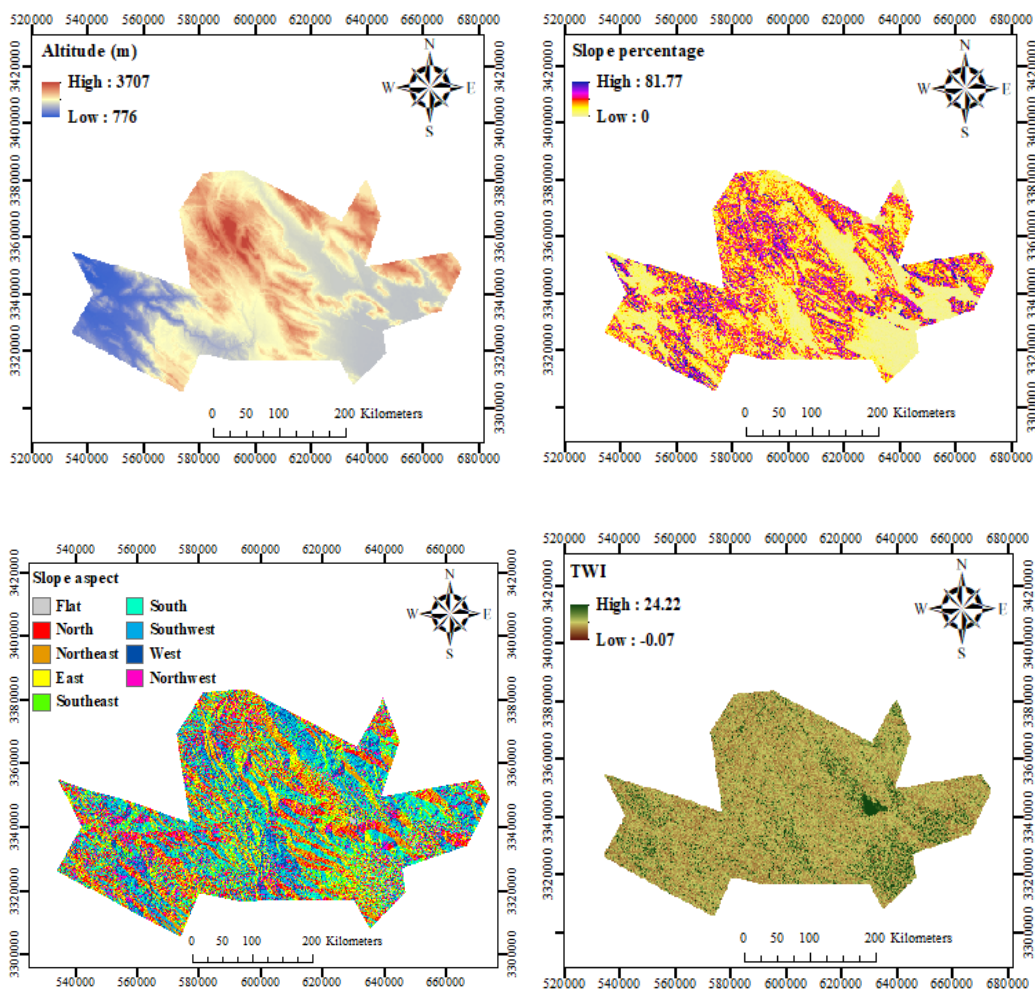
$$NDVI = \frac{B5 - B4}{B5 + B4} \quad (1)$$

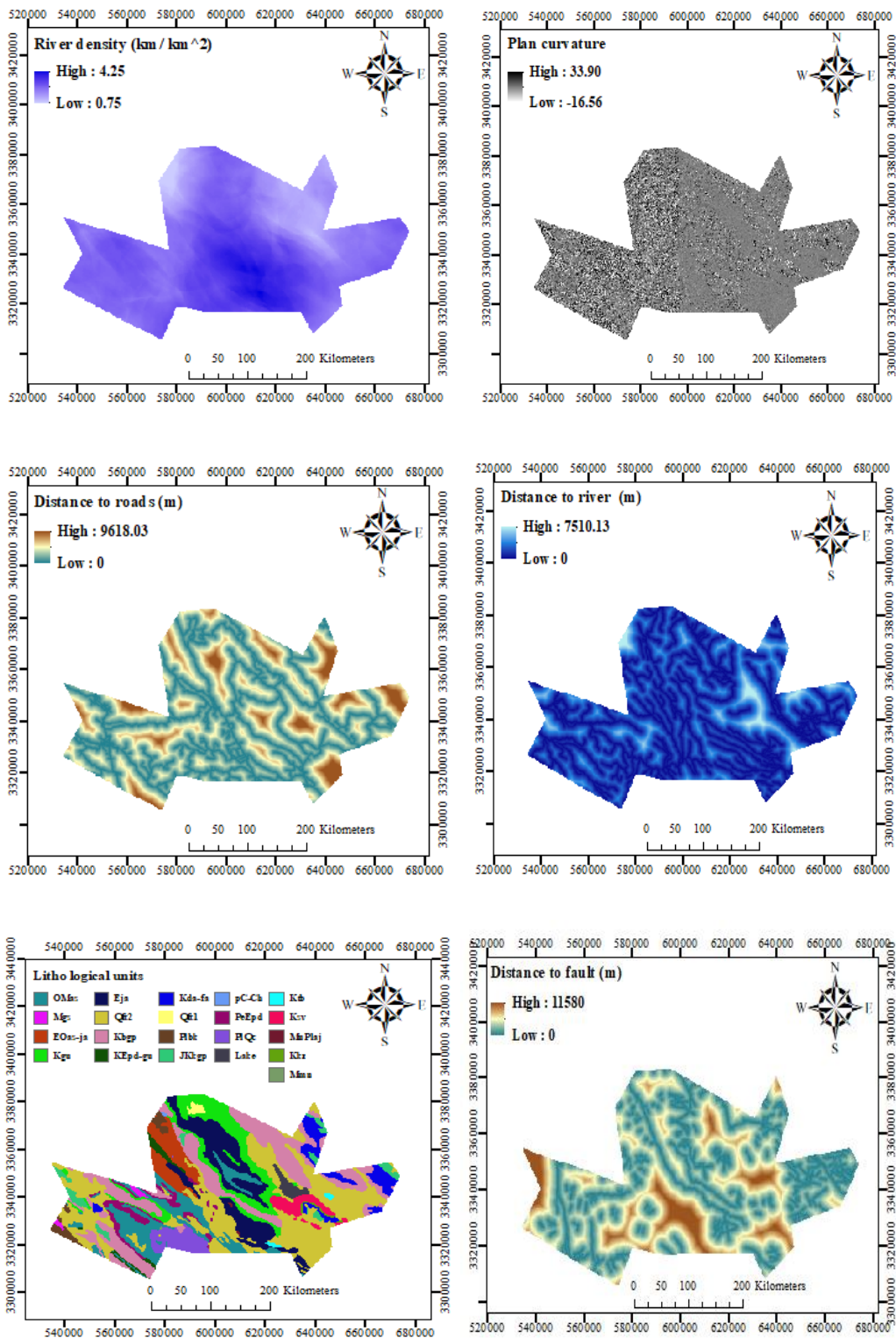
where B5= NIR and B4= Red, NIR and Red are the infrared and red portions of the electromagnetic spectrum, respectively.

Annual mean rainfall (AMR)

Rainfall is considered to be the most common cause of landslides, and rainfall-triggered landslides have caused

significant damage to agricultural lands, communication infrastructure, production of rangeland biomass and other properties, and the Earth's thrust level is saturated from the bottom (Lumb, 1975; Duc, 2012). The annual mean rainfall data were obtained from the Fars Regional Water Organization in-2001-2018 and the annual mean rainfall map was prepared using the inverse distance weighting (IDW) interpolation method (Hong et al., 2016) (Fig. 3).





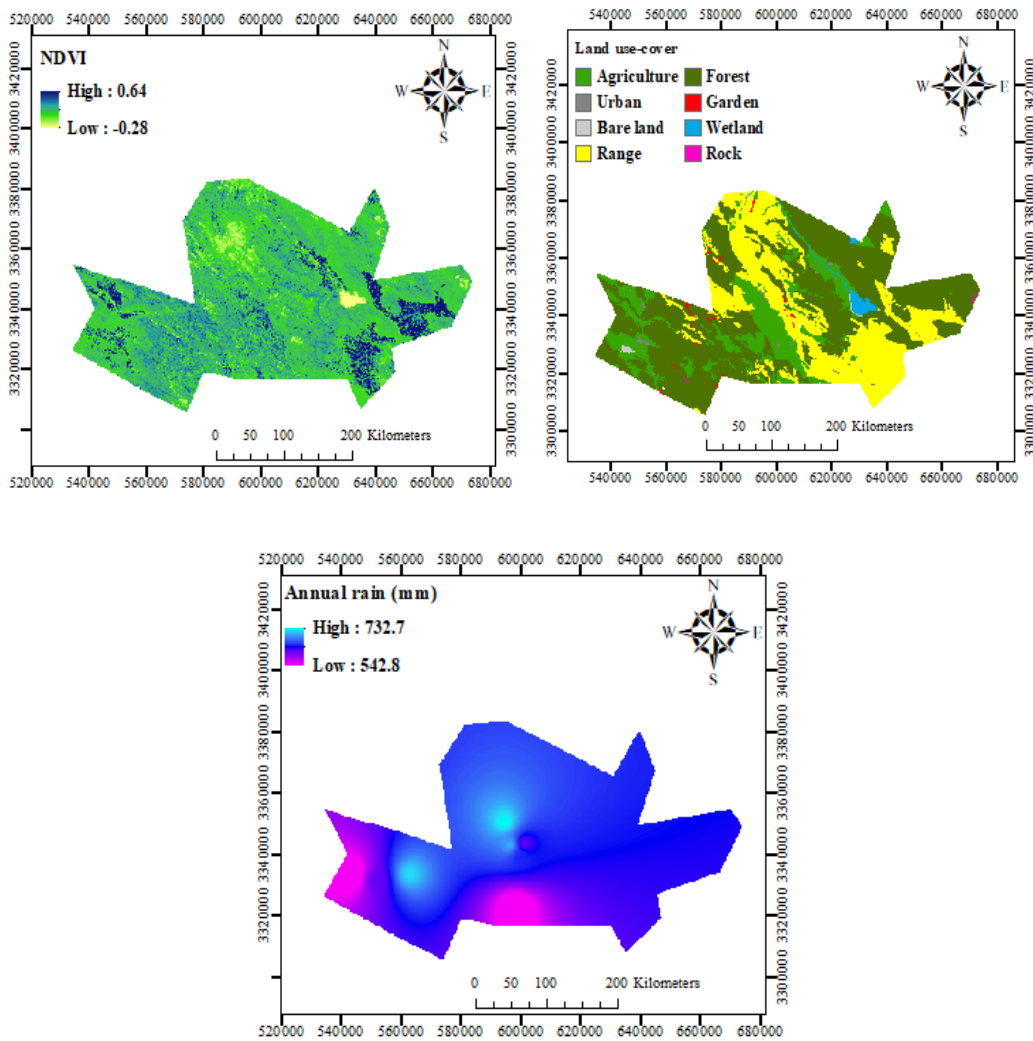


Fig. 3. Landslide effective factor maps used in this study.

Assignment of weighting effective factors using AHP

The hierarchical analysis process is one of the most famous multi - attribute decision - making techniques (Bowen, 1993). AHP is a measurement concept of a pairwise comparison matrix (PCM) and is based on the judgment of experts to obtain the priority weight. The PCM is calculated based on weights 1 to 9 (Table 2), which shows the importance of the map to other points (Saaty, 1999). The main principle for comparing order is that a consistency ratio (CR) of exactly 0.1, which does not indicate a

satisfactory matrix, and a ratio higher than 0.1 indicates that the PCM should be changed (Mundalik et al., 2018). The CI was calculated as follows:

$$CI = \lambda_{max} - n / n-1 \tag{2}$$

Where n represents the number of rows or columns in the comparison matrix (number of criteria). If the adjustment factor is equal to or less than 0.1, compatibility is required in arbitration (Malczewski, 1999). The coefficient in the present study was less than 0.1 (0.05) which was acceptable.

Table 2. AHP scale (Saaty, 2008).

Scale	1	2	3	4	5	6	7	8	9
Importance	Equal	Weak	Moderate	Moderate plus	Strong	Strong plus	Very strong	Very, very strong	Extreme

Maximum entropy (MaxEnt) algorithm

The MaxEnt model is a machine learning-based data mining technique that assesses the likelihood of risk distribution in relation to environmental factors using presence-only points/locations of hazards (Phillips et al., 2006; Yang et al., 2013). This model has a general method for estimating the probability distribution of hazards that has been proven in practical studies (Elith et al., 2006; Yost et al., 2008).

Model evaluation method

To evaluate the accuracy of the built models, a receiver operating characteristic (ROC) curve was used (Chang-Jo and Fabbri, 2003). In other words, the area below the ROC (AUC) curve is useful for quantifying uncertainty in model predictions (Zipkin et al., 2012). Predictive performance is an essential step for model accuracy in predicting a validation data set (30% of the points do not use the training process) (Tien Bui et al., 2012). In short, the most ideal model has the highest AUC and values (AUC) ranging from 0.5 to 1 (Yesilnacar, 2005).

Results

Multicollinearity Analysis (McA)

Tolerance (TOL) and VIF indices were used for multicollinearity evaluation among the effective factors (Table. 3). In this study, there was a

negative correlation between tolerance and VIF indices (Hong et al., 2016; Wang et al., 2019). Therefore, according to the table, there is no VIF value above 10 or the TOL value is <0.1 , because these two indicators represent collinearity among layers. Therefore, the use of 13 controllers' variable landslides is permitted in the modeling process. Quantitative and qualitative factor layers were introduced into the MaxEnt environment in ASCII format and CSV landslide inventories.

Determining the important parameters on which the landslide occurred

In the present study, the AHP method was used to investigate the weighting and determine the important parameters in the occurrence of landslides in the northern part of Fars Province. The AHP results are summarized in Table. 4. As shown in the table, in this study, 13 layers affecting the landslide sensitivity were used (e.g., (Lu), (LU-C), (S_P), (S_A), altitude, (Plan-C), (TWI), (DT_R), (DT_{RS}), (DT_F), (RD), (NDVI) and (AR)). (Lu), (LU-C), and (SP) variables have the first to third ranks in importance/ value on the occurrence of landslides in the study area, respectively, and the (SA), altitude, (Plan-C), (TWI), (DTR), (DTRS), (DTF), river density (RD), (NDVI), (AMR), (Lu) and (LU-C) variables have the fourth to thirteenth rank in terms of significance on the landslide events.

Table 3. Multicollinearity analysis for the landslide affecting factors.

Model	Coefficients ^a				Collinearity Statistics		
	Unstandardized Coefficients		Standardized Coefficients	t	Sig.	Tolerance	VIF
	B	Std. Error	Beta				
(Constant)	-4.361	1.077		-4.051	0.000		
Altitude	-8.694E-5	0.000	-0.067	-0.801	0.425	0.856	1.168
Distance to river	-8.978E-5	0.000	-0.178	-2.040	0.044	0.796	1.257
River density	0.117	0.074	0.138	1.579	0.117	0.797	1.255
Distance to roads	-7.092E-5	0.000	-0.234	-2.730	0.007	0.826	1.211
Slope percentage	0.008	0.005	0.155	1.849	0.067	0.866	1.155
TWI	-0.008	0.018	-0.040	-0.468	0.641	0.833	1.201
Slope aspect	-0.014	0.020	-0.057	-0.704	0.483	0.934	1.071
Distance to fault	-3.411E-7	0.000	-0.001	-0.015	0.988	0.896	1.116
Litho logical units	-0.007	0.015	-0.040	-0.469	0.640	0.832	1.202
Land use-cover	0.037	0.027	0.125	1.390	0.167	0.754	1.326
NDVI	-0.120	0.596	-0.017	-0.201	0.841	0.900	1.111
Plan curvature	0.152	0.093	0.137	1.640	0.104	0.866	1.154
Annual rain	0.007	0.001	0.421	4.881	0.000	0.816	1.226

Table 4. Weights of layers using AHP.

Factors	Litho logical units	Land use-cover	Slope percentage	Slope aspect	Altitude	Plan curvature	TWI	Distance to river	Distance to roads	Distance to fault	River density	NDVI	Annual rain
AHP	0.223	0.169	0.134	0.107	0.083	0.066	0.055	0.047	0.033	0.030	0.021	0.017	0.014

Landslide Occurrence Mapping (LOM)

The sensitivity map for sliding and each data set in the study area were prepared using a continuous and categorical data set with 10,000 background samples. Finally, the ME model uses three sets of samples (i.e., R1, R2, R3) in the repetition phase. In addition, the first replicate field was

selected by default, which was performed in the present study in three repetitions (1, 2 and 3). Landslide occurrence mapping of the case study using three groups of repetitions is presented in Fig. 4. The predictive results of landslide occurrence were transformed into a raster format and opened in ArcGIS. Then employing the raster map, the landslide susceptibility

map was isolated and visualized using four categories based on Quantile method, like number landslide "Low, Moderate, High and Very high" (Fig. 5) (Razandi et al., 2015; Naghibi and Pourghasemi, 2015). On the other hand, the percentage of risk areas of landslides in all three groups of data replication is shown in Table 5. According to the table, the highest percentage of landslide sensitivity class area is located in the study area in the moderate class (%26.14) with once repetition and using the maximum entropy model, and the highest landslide

sensitivity was observed in the high, very high and low classes, respectively. In addition, in the second and third repetitions, the highest sensitivity of landslides was in the moderate-sensitivity class. According to the landslide sensitivity scale, the highest sensitivity occurred in high, very high and low classes in the second iteration and most landslides after the moderate class, in high, low, and very high classes was observed in the third iteration with a small percentage difference.

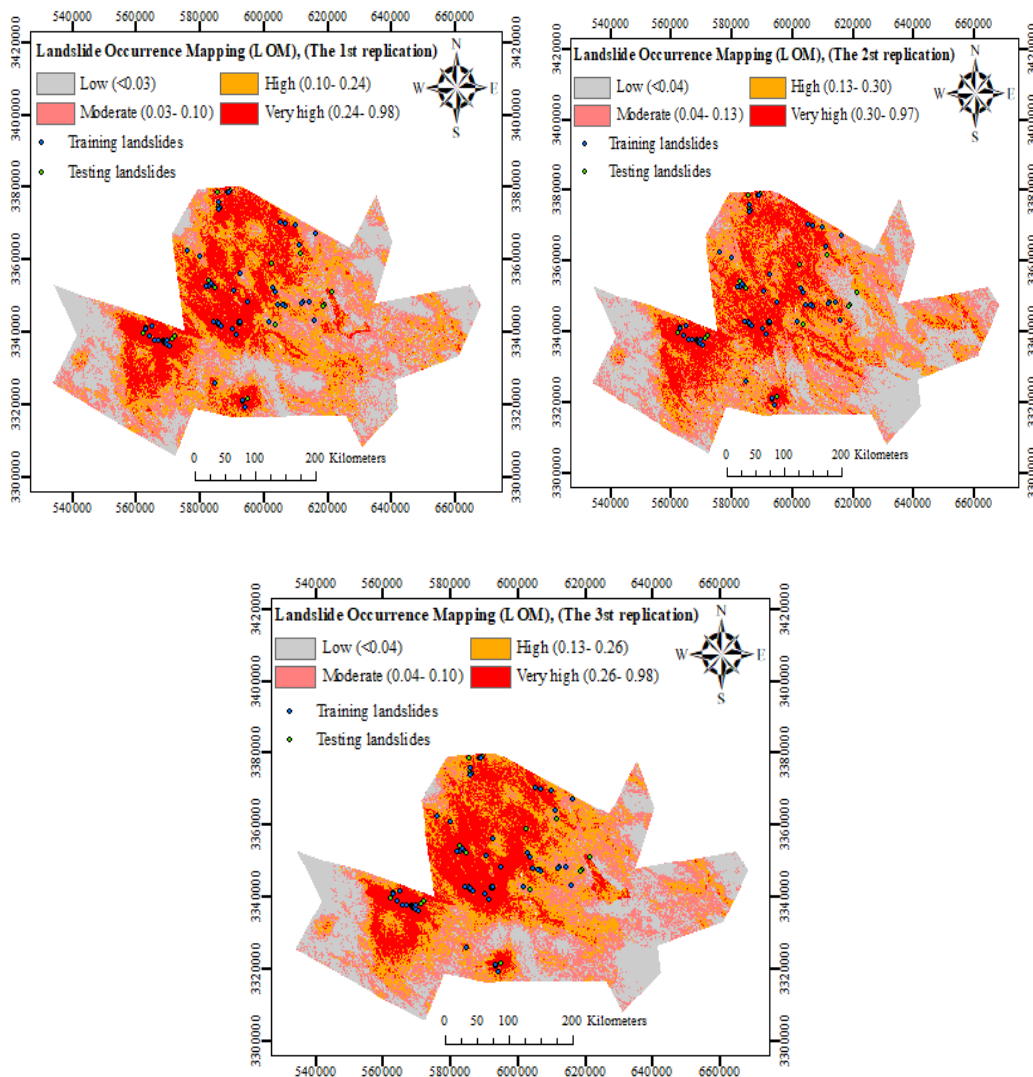


Fig. 4. Landslide susceptibility map derived from the Maximum Entropy model.

Table 5. Area percentage of models' classes.

Landslide hazard classes	The first repetition Class area (%)	Landslide hazard classes	The second repetition Class area (%)	Landslide hazard classes	The third repetition Class area (%)
Low (<0.03)	24.20	Low (<0.04)	23.71	Low (<0.04)	24.75
Moderate (0.03- 0.10)	26.14	Moderate (0.04- 0.13)	25.91	Moderate (0.04- 0.10)	25.71
High (0.10- 0.24)	25.00	High (0.13- 0.30)	25.33	High (0.10- 0.26)	24.91
Very high (0.24- 0.98)	24.63	Very high (0.30- 0.97)	25.03	Very high (0.26- 0.98)	24.61
Totally	100	Totally	100	Totally	100

Maximum entropy performance

Landslide sensitivity event validation should be used as a reference for the performance of the algorithms used. Accreditation was used to perform sensitivity analysis for individual algorithms and a combination of algorithms in which different mapping methods were tested (Remondo et al., 2003; Chung and Fabbri, 2003). As mentioned earlier, the Maxent model was implemented using three sampling strategies. According to the obtained

results, the most accurate training data among the three repetition groups, the first repetition had the highest accuracy (0.904) and the third and second repetitions (0.898 and 0.892) had the highest accuracy. On the other hand, the highest accuracy in predicting the risk of landslides using the maximum entropy model and testing dataset, among the three repetitions, the third, second and first repetitions were the most accurate (0.778, 0.770 and 0.640), respectively.

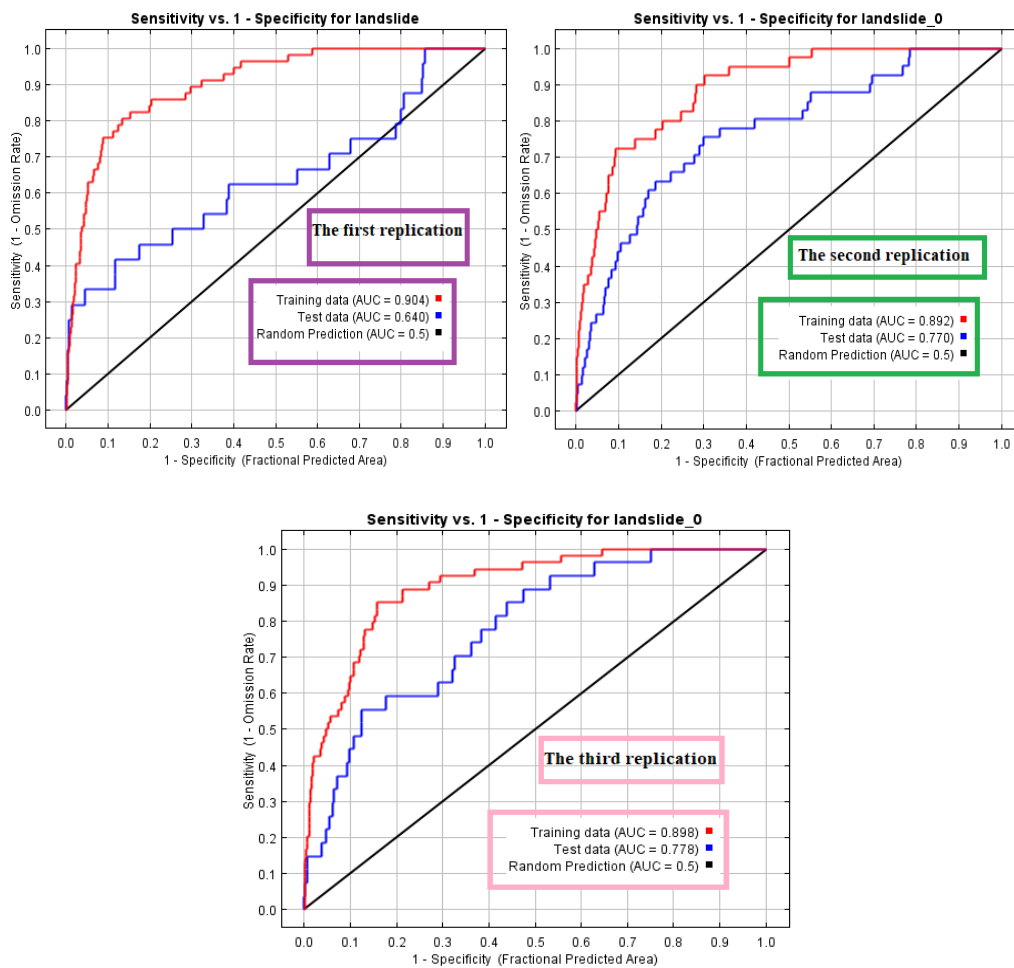


Fig. 5. The ROC curves of three groups of datasets for landslide.

Discussion

Spatial prediction of landslides is an important issue in the science of geomorphology and natural hazards. Understanding the factors that cause landslides is essential for effective risk management (He et al., 2019). Researchers believe that machine learning techniques can solve many real-world problems compared to conventional methods (Shahabi and Hashim, 2015). Shirzadi et al. (2011) showed that the clarity of the sample method and size is appropriate for understanding the accuracy of prediction in shallow slips. For this reason, research on natural hazards has been associated with the use of new

techniques and approaches such as machine learning (Pourghasemi et al., 2019), fuzzy ANP approaches (Alilo et al., 2019), Dm-Chameleon clustering algorithm (Hu et al., 2019), Google Earth for mapping (Rabby and Li, 2019), traditional aerial photography (Koca and Koca, 2019), and remote sensing techniques (Zhao et al., 2018). Prediction through modeling and simulation is now considered one of the important goals of natural resource studies because it is often thought that decision making by planners and engineers is sufficient. For this reason, this process must be performed carefully and precisely (Pourghasemi and Rahmati, 2018). Yilmaz (2010) stated that the use of statistical models

in the process of inputs, outputs and spatial analysis is time consuming, while machine learning has the advantage of automatically recognizing the interaction of dependent and independent variables. Therefore, machine learning is relatively easy, and predictive accuracy usually goes beyond more common methods (e.g., analytic hierarchical process, statistical methods) if there is a complex interaction (Tien Bui et al., 2012). Our results complement the results of Felicísimo et al. (2013), who used different models of machine learning, including multiple logistic regression. (MLR), MARS, CART and Yousef et al. (2016), who used RF, BRT, GLM and CART techniques to assess landslide sensitivity and then compared their performance. In the present study, a machine learning method, i.e., maximum entropy models, has been performed to Landslide Occurrence Mapping (LOM). Because understanding the factors that cause landslides is essential for effective risk management (Hong et al., 2019), in this study, 13 factors influencing landslide risk have been used, including lithological units (Lu), land use cover (LU-C), slope percentage (S_P), slope aspect (S_A), altitude, plan curvature (Plan-C), topographic wetness index (TWI), distance to river (DT_R), distance to roads (DT_{RS}), distance to fault (DT_F), river density (RD), normalized difference vegetation index (NDVI) and annual rain (AR) in the north of Fars Province. In general, strong linear changes and correlations between independent variables interfere with statistical models to a lesser degree (Chen et al., 2019). This test has two factors: tolerance and variance inflation factors (VIF). Therefore, appraising a multi-collinearity study of the affecting variables the occurrence of landslides can be useful in the study area. This is because it reduces the multicollinearity between the independent variables and reduces the model error. Therefore,

in our research, there is no multicollinearity between the factors and all the factors have been used for modeling. For this reason, all layers have $TOL > 0.1$ and $VIF < 10$. Affecting factors landslides were identified by various analyses in the identification of mathematical maps using the integrated AHP method and geological technology. In the present study, the AHP algorithm was used to evaluate the importance of factors and to analyze the contribution of the variables. In addition, many researchers have used many methods to invest and defect the importance of factors influencing landslides, such as the LVQ algorithm, Gini and statistical sensitivity models to calculate the weight of predictor variables depending on the landslide data set (Blahut et al., 2010; Guzzetti et al., 2012). Factors affecting landslide sensitivity were identified by various analyses in the identification of mathematical maps using the integrated AHP method and geological technology (Rajasekhar et al., 2019). Shows the final weight of each of the effective layers and compares them lithological units (Lu), land use-cover (LU-C), slope percentage with numbers of 0.223, 0.169 and 0.134, respectively have the most importance on the landslide risk in the case study; on the other hand, the lowest weight was obtained for annual rain (0.014). The value of the consistency ratio (CR) is 0.05, which is considered compatible and thus reduces any mentality that CR differs in different studies, such as the research of Rajasekhar et al. (2018) They have a consistency ratio of 0.08 which should be $CR < 0.1$. Pourghasemi and Rahmati (2018) state overall, classified layers, such as slope aspect and land use, have relatively strong effects on landslides. Although different machine learning models have been used to map landslide sensitivity, the accuracy of predicting these methods is still debated (Tien Bui et al., 2016). On the other hand, it has

been well established that choosing the best model among the various machine learning techniques plays an important role in assessing landslide sensitization (Felicísimo et al., 2013). Although some machine learning features the same model accuracy, they are unique in their individual approaches to modeling landslide sensitivity and determining the relationships between geological factors and the onset of landslides (Goetz et al., 2015). Understanding and being aware of these important issues is essential for applying a suitable model for a specific purpose or for a specific study area (Brenning, 2008). In the present study, three groups of repetitions were used to prepare a landslide risk map, where most of the landslide risk had the second repetition because the highest risk of landslides occurred on the very high-risk floor (25.03) and in two repetitions in the three repetition groups and many landslides occurred in the central and northern regions of the case study. Because landslide sensitivity is a widespread natural hazard, data mining methods can predict landslide-prone areas. In the present study, this issue is investigated by evaluating the maximum entropy model. Pandey et al. (2018) used the maximum entropy model to evaluate the susceptibility to landslides and reported that this model has a good forecast of 0.78 AUC. Arabamari et al. (2019) used six models to predict the occurrence of landslides and reported that collection models such as SI-LDR, AHP-SI and AHP-LDR had higher prediction values than the SI, LDA and AHP models. In this study, this maximum entropy method provides quantitative results and allows us to compare the results with those of other studies around the world. The concept of maximizing the entropy of information theory (Banavar et al., 2010; Ruddell et al., 2013). This concept requires the creation of a possible model prediction that uses the minimum information obtained instead

of all available data (Phillips et al., 2006). This information is useful for predicting spatial patterns with the highest precision. Effective variables also show their interaction and the observed ground drift distributions show the location without the initial statistical hypothesis. Recently, Pourghasemi et al. (2017) evaluated machine learning methods (ANN-ME, ANN-SVM, SVM-ME) and individual (MaxEnt, ANN, SVM) for gully erosion. They illustrated that the maximum entropy algorithm had the lowest value in terms of agreement with the algorithms. The accuracy of the training data was the highest in the first iteration (AUC=0.904) of the present study and the Maximum entropy accuracy in predicting landslide risk was mapped with three repetitions. Maxent is a machine-learning model aimed only at public presence (Phillips et al., 2006). The only feature of the presence of the model can be considered an advantage in remote and unbearable areas (Pearson et al., 2007). This feature is especially important for landslide studies because even if there is no phenomenon, the possibility of landslides cannot be ruled out. In other words, it is possible that an area without landslides has a high potential for occurrence, but morphological evidence has not yet emerged spatially or cannot be properly captured by the researcher. Therefore, using the maximum entropy model, as a method that depends on the locations of presence in the landslide, can eliminate many of these cases in terms of efficiency. However, this feature allows the model to be exposed to biased data (Cao et al., 2016), where attendance data are often recorded near accessible locations (McCarthy et al., 2011).

Conclusions

Identified using a regional-scale modern machine learning model is necessary for accurate and precise

monitoring and assessment of land degradation, as well as for sustainable land management in humid climates. The Spatial distribution of landslides was recorded and predicted in an effective way. This is important for achieving sustainable development on earth by increasing the population and land use, which will lead to sustainable long-term development if impossible. The present research can effectively contribute to the UN goal of sustainable development and the neutralization of land degradation. Landslide sensitivity mapping plays an important role in providing a platform for decision makers and officials, especially in landslide-prone areas. The present study was performed using the Maxent machine learning model in the critical region of northern Fars Province, Iran. Hence, 13 controlling factors on landslide sensitivity, namely (Lu), (LU-C), (S_P), (S_A), altitude, (Plan-C), (TWI), (DT_R), (DT_{RS}), (DT_F), (RD), (NDVI) and (AMR). There was no multicollinearity among the effective factors and the litho logical units (Lu), land use cover (LU-C), and slope

percentage (S_P) were the most important factors affecting landslide events in the case study. 25.03% of the area occurs on the very high risk of landslides. Of the three repetition groups, the third iteration was the most accurate in predicting landslides using the testing data. The accuracy of predicting the maximum entropy model in the present study is good for the risk of landslides. The results of the present study are consistent with Phillips et al. (2006), Liu et al. (2012), Vorpahl et al. (2012), Felicísimo et al. (2013), Park (2015), Hong et al. (2016), Kornejady et al. (2017), in courses with maximum allowable maximum entropy model performance. Finally, it is recommended to use other methods of landslide sensitivity for various reasons. The results of this research can be used for optimal management of the region by the Crisis Management Organization and the officials of the General Department of Natural Resources of Fars Province. In addition, it can be used by researchers interested in the subject of earth sensitivity.

References

1. Akgun, A., Dag, S., and Bulut, F. 2008. Landslide susceptibility mapping for a landslide-prone area (Findikli, NE of Turkey) by likelihood-frequency ratio and weighted linear combination models. *Environ. Geol.* 54: 1127-1143.
2. Alilou, H., Rahmati, O., Singh, V.P., Choubin, B., Pradhan, B., Keesstra, S., Ghiasi, S.S., and Sadeghi, S.H. 2019. Evaluation of watershed health using Fuzzy-ANP approach considering geo-environmental and topo-hydrological criteria. *J. Environ. Manag.* 232: 22-36.
3. Arabameri, A., Pradhan, B., Rezaei, K., Lee, S., and Sohrabi, M. 2019. An ensemble model for landslide susceptibility mapping in a forested area. *Geocarto Int.* pp. 1-25.
4. Banavar, J.R., Maritan, A., and Volkov, I. 2010. Applications of the principle of maximum entropy: from physics to ecology. *J. Phys. Condens. Matter.* 22 (6), 063101.
5. Beguería, S. 2006. Changes in land cover and shallow landslide activity: a case study in the Spanish Pyrenees. *Geomorphology.* 74: 196-206.
6. Blahut, J., Van Westen, C.J., and Sterlacchini, S. 2010. Analysis of landslide inventories for accurate prediction of debris-flow source areas. *Geomorphology.* 119 (1-2): 36-51. <https://doi.org/10.1016/j.geomorph.2010.02.017>.
7. Blaschke, T., and Montanarella, L. (Eds.), SAGA - Seconds Out (=Hamburger Beiträge zur Physischen Geographie und Landschaftsökologie, 19), pp. 23-32.
8. Bordoni, M., Meisina, C., Valentino, R., Bittelli, M., and Chersich, S. 2015.

- Site-specific to local-scale shallow landslides triggering zones assessment using TRIGRS. *Nat. Hazards Earth Syst. Sci.* 15p.
9. Boubli, J.P., and De Lima, M.G. 2009. Modeling the geographical distribution and fundamental niches of *Cacajao* spp. and *Chiropotes israelita* in Northwestern Amazonia via a maximum entropy algorithm. *International Journal of Primatology*, 30 (2): 217-228.
 10. Bowen, W.M. 1993. AHP: Multiple Criteria Evaluation in Klosterman. New Brunswick: Center for Urban Policy Research.
 11. Brardinoni, F., Slaymaker, O., and Hassan, M.A. 2003. Landslide inventory in a rugged forested watershed: a comparison between air-photo and field survey data, *Geomorphology*, 54: 179-196.
 12. Brenning, A. 2008. Statistical geocomputing combining R and SAGA: the example of landslide susceptibility analysis with generalized additive models. In: Böhner, J.
 13. Broeckx, J., et al. 2016. Linking landslide susceptibility to sediment yield at regional scale: application to Romania. *Geomorphology*. 268: 222-232.
 14. Bui, D.T., et al. 2015. A novel hybrid evidential belief function-based fuzzy logic model in spatial prediction of rainfall-induced shallow landslides in the Lang Son city area (Vietnam). *Geomat. Nat. Haz. Risk*. 6: 243-271.
 15. Cao, B., Bai, C., Zhang, L., Li, G., and Mao, M. 2016. Modeling habitat distribution of *Cornus officinalis* with Maxent modeling and fuzzy logics in China. *J. Plant Ecol.* rtw009.
 16. Chang-Jo, F.C., and Fabbri, A.G. 2003. Validation of spatial prediction models for landslide hazard mapping. *Natural Hazards*, 30 (3): 451-472.
 17. Chen, W., Li, X., Wang, Y., Chen, G., and Liu, S. 2014. Forested landslide detection using LiDAR data and the random forest algorithm: a case study of the Three Gorges, China. *Remote Sens. Environ.* 152: 291-301.
 18. Chen, W., Pourghasemi, H.R., and Naghibi, S.A. 2017. Prioritization of landslide conditioning factors and its spatial modeling in Shangnan County, China using GIS-based data mining algorithms. *Bull. Eng. Geol. Environ.* pp. 1-19.
 19. Chen, W., Shahabi, H., Shirzadi, A., Li, T., Guo, C., Hong, H., Li, W., Pan, D., Hui, J., Ma, M., Xi, M., and Ahmad, B.B. 2018. A novel ensemble approach of bivariate statistical-based logistic model tree classifier for landslide susceptibility assessment. *Geocarto Int.* 33 (12): 1398-1420.
 20. Chen, W., Panahi, M., Tsangaratos, P., Shahabi, H., Ilija, I., Panahi, S., Li, Sh., Jaafari, A., and Ahmad, B.B. 2019. Applying population-based evolutionary algorithms and a neuro-fuzzy system for modeling landslide susceptibility. *Catena* 172: 212-231. <https://doi.org/10.1016/j.catena.2018.08.025>.
 21. Chung C.J.F., and Fabbri, A.G. 2003. Validation of spatial prediction models for landslide hazard mapping. *Nat Hazards*. 30(3): 451-472. doi:10.1023/B: NHAZ.0000007172.62651.2b.
 22. Costanza, J., Beck, S., Pyne, M., Terando, A., Rubino, M., White, R., and Collazo, J. 2016. Assessing Climate-Sensitive Ecosystems in the Southeastern United States (No. 2016-1073). US Geological Survey.
 23. Dou, J., et al. 2015. An integrated artificial neural network model for the landslide susceptibility assessment of Osado Island, Japan. *Nat. Hazards*, 78: 1749-1776.
 24. Duc, D.M. 2012. Rainfall-triggered large landslides on 15 December 2005 in Van Canh District, Binh Dinh Province, Vietnam. *Landslides*, 10: 219-230.
 25. Elith, J.H., Graham, C.P., Anderson, R., Dudík, M., Ferrier, S., Guisan, A.J., Hijmans, R., Huettmann, F.R., Leathwick, J., Lehmann, A., et al. 2006. Novel methods improve prediction of species' distributions from occurrence data. *Ecography*, 29: 129-151.
 26. Elkadiri, R., Sultan, M., Youssef, A., Elbayoumi, T., Chase, R., Bulkhi, A., and Al-Katheeri, M. 2014. A remote sensing-based approach for debris-flow susceptibility assessment using artificial neural networks and logistic regression modeling. *Selected topics in applied earth observations and remote sensing*, IEEE J. Sel. Top. Appl. Earth Obs.

- Remote Sens. doi:10.1109/JSTARS.2014.2337273.
27. Erenner, A., and Düzgün, H.S.B. 2010. Improvement of statistical landslide susceptibility mapping by using spatial and global regression methods in the case of More and Romsdal (Norway). *Landslides*, 7 (1): 55–68.
28. Felicísimo, A., Cuartero, A., Remondo, J., and Quirós, E. 2013. Mapping landslide susceptibility with logistic regression, multiple adaptive regression splines, classification and regression trees, and maximum entropy methods: a comparative study. *Landslides*, 10: 175-189.
29. Fukuoka, M. 1980. Landslides associated with rainfall. *Geotech. Eng.* 11 (1).
30. Galli, M., Ardizzone, F., Cardinali, M., Guzzetti, F., and Reichenbach, P. 2008. Comparing landslide inventory maps. *Geomorphology*, 94 (3): 268-289.
31. Galli, M., Ardizzone, F., Cardinali, M., Guzzetti, F., and Reichenbach, P. 2008. Comparing landslide inventory maps. *Geomorphology*, 94: 268-289.
32. Guzzetti, F., Cesare, A., Cardinali, M., Fiorucci, F., Santangelo.
33. He, Q., Shahabi, H., Shirzadi, A., Li, S., Chen, W., Wang, N., ... Ahmad, B.B. 2019. Landslide spatial modelling using novel bivariate statistical based Naïve Bayes, RBF Classifier, and RBF Network machine learning algorithms. *Science of the Total Environment*. doi: 10.1016/j.scitotenv.2019.01.329.
34. Hong, H., Naghibi, S.A., Pourghasemi, H.R., and Pradhan, B. 2016. GIS-based landslide spatial modeling in Ganzhou City, China. *Arab. J. Geosci.* 9 (2): 1-26.
35. Hong, H., Pourghasemi, H.R., and Pourtaghi, Z.S. 2016. Landslide susceptibility assessment in Lianhua County (China): a comparison between a random forest data mining technique and bivariate and multivariate statistical. *Geomorphology*, 259: 105-118.
36. Hu, J., Zhu, H., Mao, Y., Zhang, C., Liang, T., and Mao, D. 2019. Using uncertain DM chameleon clustering algorithm based on machine learning to predict landslide hazards. *J. Robot. Mechatron.* 31 (2): 329-338.
37. Kayastha, P., Dhital, M.R., and De Smedt, F. 2012. Landslide susceptibility mapping using the weight of evidence method in the Tinau watershed, Nepal. *Nat. Hazards*. 63: 479-498.
38. Koca, T.K., and Koca, M.Y. 2019. Volume estimation and evaluation of rotational landslides using multi-temporal aerial photographs in Çaglayan dam reservoir area, Turkey. *Arabian J. Geosci.* 12 (5): 140.
39. Komac, M. 2006. A landslide susceptibility model using the Analytical Hierarchy Process method and multivariate statistics in perialpine Slovenia, *Geomorphology*, 74: 17-28.
40. Kornejady, A., Ownegh, M., and Bahremand, A. 2017. Landslide susceptibility assessment using maximum entropy model with two different data sampling methods. *Catena* 152: 144–162. doi: 10.1016/j.catena.
41. Leventhal, A.R., and Kotze, G.P. 2008. Landslide susceptibility and hazard mapping in Australia for land-use planning - with reference to challenges in metropolitan suburbia. *Eng. Geol.* 102 (3-4): 238-250.
42. Liu, J., et al. 2004. Landslide hazard assessment in the Three Gorges area of the Yangtze River using ASTER imagery: Zigui–Badong. *Geomorphology*. 61: 171-187.
43. Liu, Y., Guo, Q., and Tian, Y. 2012. A software framework for classification models of geo graphical data. *Comput. Geosci.* 42: 47-56.
44. Lopez, R.P., Larrea-Alcazar, D., and Zenteno-Ruiz, F. 2011. Spatial pattern analysis of dominant species in the Prepuna: Gaining insight into community dynamics in the semi-arid, subtropical Andes. *J. Arid Environ.* 74: 1534-1539.
45. Lumb, P. 1975. Slope failure in Hong Kong. *Q. J. Eng. Geol.* 8: 31-65.
46. McCarthy, E., Moretti, D., Thomas, L., DiMarzio, N., Morrissey, R., Jarvis, S., ... Dilley, A. 2011. Changes in spatial and temporal distribution and vocal behavior of Blainville's beaked whales (*Mesoplodon densirostris*) during multiship exercises with mid-frequency sonar. *Mar. Mamm. Sci.* 27 (3): 206-226.

47. Meinhardt, M., Fink, M., and Tunschel, H. 2015. Landslide susceptibility analysis in central Vietnam based on an incomplete landslide inventory: comparison of a new method to calculate weighting factors by means of bivariate statistics. *Geomorphology*, 234: 80-97.
48. Michele, Ch., and Kang-tsung, 2012. Landslide inventory maps: new tools for an old problem. *Earth-Sci. Rev.* 112 (1-2): 42-66. <https://doi.org/10.1016/j.earscirev.2012.02.001>.
49. Moreno, R., Zamora, R., Molina, J.R., Vasquez, A., and Herrera, M.Á. 2011. Predictive modeling of microhabitats for endemic birds in South Chilean temperate forests using maximum entropy (Maxent). *Ecological Informatics*, 6(6): 364-370.
50. Mundalik, V., Fernandes, C., Kadam, A.K., and Umrikar, B.N. 2018. Integrated geomorphological, geospatial and AHP technique for groundwater prospects mapping in basaltic terrain. *Hydro spatial Analysis*, 2 (1), 16-27.
51. Nasiri Aghdam, I., Varzandeh, M.H.M., and Pradhan, B. 2016. Landslide susceptibility mapping using an ensemble statistical index (Wi) and adaptive neuro-fuzzy inference system (ANFIS) model at Alborz Mountains (Iran). *Environ. Earth Sci.* 75: 1-20.
52. Nefeslioglu, H.A., Duman, T.Y., and Durmaz, S. 2008. Landslide susceptibility mapping for a part of tectonic Kelkit Valley (Eastern Black Sea region of Turkey). *Geomorphology* 94: 401-418.
53. Pandey, V.K., Sharma, K.K., Pourghasemi, H.R., and Bandooni, S.K. 2019. Sedimentological characteristics and application of machine learning techniques for landslide susceptibility modelling along the highway corridor Nahan to Rajgarh (Himachal Pradesh), India. *CATENA*, 182: 104150. doi: 10.1016/j.catena.2019.104150.
54. Pandey, V.K., Pourghasemi, H.R., and Sharma, M.C. 2018. Landslide susceptibility mapping using maximum entropy and support vector machine models along the highway corridor, Garhwal Himalaya. *Geocarto Int.* pp. 1-20.
55. Park, N.W. 2015. Using maximum entropy modeling for landslide susceptibility mapping with multiple geo environmental data sets. *Environmental Earth Sciences*, 73(3): 937-949.
56. Park, N.W., and Chi, K.H. 2008. Quantitative assessment of landslide susceptibility using high-resolution remote sensing data and a generalized additive model. *Int. J. Remote Sens.* 29: 247-264.
57. Peterson, A.T. 2006. Uses and Requirements of Ecological Niche Models and Related Distributional Models.
58. Pham, B.T., Bui, D.T., Prakash, I., and Dholakia, M. 2016. Rotation Forest fuzzy rule-based classifier ensemble for spatial prediction of landslides using GIS. *Nat. Hazards*. 83: 97-127.
59. Pham, B.T., et al. 2017. A novel ensemble classifier of rotation forest and Naïve Bayer for landslide susceptibility assessment at the Luc Yen district, Yen Bai Province (Viet Nam) using GIS. *Geomat. Nat. Haz. Risk*. 8: 649-671.
60. Phillips, S.J., Anderson, R.P., and Schapire, R.E. 2006. Maximum entropy modeling of species geographic distributions. *Ecological modelling*, 190(3-4): 231-259.
61. Pourghasemi, H.R., and Rahmati, O. 2018. Prediction of the landslide susceptibility: Which algorithm, which precision? *CATENA*, 162: 177-192. doi: 10.1016/j.catena.2017.11.022.
62. Pourghasemi, H.R., Gayen, A., Panahi, M., Rezaie, F., and Blaschke, T. 2019. Multi-hazard probability assessment and mapping with emphasis on landslides, floods, and earthquakes in Iran. *Sci. Total Environ.* <https://doi.org/10.1016/j.scitotenv.2019.07.203>.
63. Pourghasemi, H.R., and Kerle, N. 2016. Random forests and evidential belief function-based landslide susceptibility assessment in Western Mazandaran Province, Iran. *Environ. Earth Sci.* 75: 1-17.
64. Pourghasemi, H.R., Moradi, H.R., Fatemi Aghda, S.M., Gokceoglu, C., and Pradhan, B. 2014. GIS-based landslide susceptibility mapping with probabilistic likelihood ratio and spatial multi-criteria evaluation models (North of Tehran, Iran). *Arab. J. Geosci.* 7: 1857-1878.

65. Pourghasemi, H.R., Yousefi, S., Kornejady, A., and Cerda, A. 2017. Performance assessment of individual and ensemble data-mining techniques for gully erosion modeling. *Sci. Total Environ.* 609: 764-775.
66. Pradhan, B. 2010. Landslide susceptibility mapping of a catchment area using frequency ratio, fuzzy logic and multivariate logistic regression approaches. *J. Indian Soc. Remote Sens.* 38(2): 301-320.
67. Pradhan, B. 2013. A comparative study on the predictive ability of the decision tree, support vector machine and neuro-fuzzy models in landslide susceptibility mapping using GIS. *Comput. Geosci.* 51: 350-365.
68. Rabby, Y.W., and Li, Y. 2019. An integrated approach to map landslides in Chittagong Hilly Areas, Bangladesh, using Google Earth and field mapping. *Landslides*, 16 (3): 633-645.
69. Rahmati, O., Kornejady, A., Samadi, M., Deo, R.C., Conoscenti, C., Lombardo, L., Dayal, K., Taghizadeh-Mehrjardi, R., Pourghasemi, H.R., Kumar, S., and Tien Bui, D. 2019a. PMT: new analytical framework for automated evaluation of geo-environmental modelling approaches. *Science of the Total Environment*, 664: 296-311. <https://doi.org/10.1016/j.scitotenv.2019.02.017>.
70. Rajasekhar, M., Sudarsana Raju, G., Sreenivasulu, Y., and Siddi Raju, R. 2019. Delineation of groundwater potential zones in semi-arid region of Jilledubanderu river basin, Anantapur District, Andhra Pradesh, India using fuzzy logic, AHP and integrated fuzzy-AHP approaches. *Hydro Research*. doi: 10.1016/j.hydres.2019.11.006.
71. Regmi, A.D., Yoshida, K., Pradhan, B., Pourghasemi, H.R., Khumamoto, T., and Akgun, A. 2014. Application of frequency ratio, statistical index and weights-of-evidence models, and their comparison in landslide susceptibility mapping in Central Nepal Himalaya. *ArabJ Geosci.* 7(2): 725-742. doi:10.1007/s12517-012-0807-z.
72. Remondo, J., González, A., Díazde Terán, J.R., Cendrero, A., Fabbri, A., and Chung, C.J.F. 2003. Validation of landslide susceptibility maps; examples and applications from a case study in Northern Spain. *Nat. Hazds.* 30(3): 437-449. doi:10.1023/B: NHAZ. 0000007201.80743.fc.
73. Ruddell, B.L., Brunzell, N.A., and Stoy, P. 2013. Applying Information Theory in the Geosciences to quantify process uncertainty, feedback, Scale. *Eps.* 94: 56-57.
74. Saaty, T.L. 1990. Decision making for leaders: the analytic hierarchy process for decisions in a complex world. RWS publications.
75. Shahabi, H., Hashim, M., and Ahmad, B.B. 2015. Remote sensing and GIS-based landslide susceptibility mapping using frequency ratio, logistic regression, and fuzzy logic methods at the central Zab basin, Iran. *Environ. Earth Sci.* 73: 1-22.
76. Shahabi, H., Khezri, S., Ahmad, B.B., and Hashim, M. 2014. Landslide susceptibility mapping at central Zab basin, Iran: a comparison between analytical hierarchy process, frequency ratio and logistic regression models. *Catena.* 115: 55-70.
77. Shirzadi, A., et al. 2017. Rock fall susceptibility assessment along a mountainous road: an evaluation of bivariate statistic, analytical hierarchy process and frequency ratio. *Environ. Earth Sci.* 76: 152.
78. Shirzadi, A., Solaimani, K., Roshan, M.H., Kavian, A., Chapi, K., Shahabi, H., Keesstra, S., Ahmad, B.B., and Bui, D.T. 2011. Uncertainties of prediction accuracy in shallow landslide modeling: sample size and raster resolution. *Catena.* 178: 172-188.
79. Tien Bui, D., Tuan, T.A., Klempe, H., Pradhan, B., and Revhaug, I. 2016. Spatial prediction models for shallow landslide hazards: a comparative assessment of the efficacy of support vector machines, artificial neural networks, kernel logistic regression, and logistic model tree. *Landslides.* 13: 361-378.
80. Trigila, A., Iadanza, C., Esposito, C., and Scarascia-Mugnozza, G. 2015. Comparison of Logistic Regression and Random Forests techniques for shallow landslide susceptibility assessment in Giampileri (NE Sicily, Italy), *Geomorphology*, 249: 119-136.

81. Tsangaratos, P., and Iliu, I. 2016. Landslide susceptibility mapping using a modified decision tree classifier in the Xanthi Prefecture, Greece. *Landslides*. 13: 305-320.
82. Tsangaratos, P., Iliu, I., Hong, H., Chen, W., and Xu, C. 2017. Applying Information Theory and GIS-based quantitative methods to produce landslide susceptibility maps in Nancheng County, China. *Landslides* 14: 1091-1111.
83. Vapnik, V.N., and Vapnik, V. 1998. *Statistical Learning Theory*. Wiley, New York.
84. Wang, Q., Li, W., Chen, W., and Bai, H. 2015. GIS-based assessment of landslide susceptibility using certainty factor and index of entropy models for the Qianyang County of Baoji city, China. *J. Earth Syst. Sci.* 124 (7): 1399-1415.
85. Wang, Y., Fang, Z., and Hong, H. 2019. Comparison of convolutional neural networks for landslide susceptibility mapping in Yanshan County, China. *Science of the Total Environment*. doi: 10.1016/j.scitotenv.2019.02.263.
86. Yalcin, A., Reis, S., Aydinoglu, A.C., and Yomralioglu, T. 2011. AGIS-based comparative study of frequency ratio, analytical hierarchy process, bivariate statistics and logistics regression methods for landslide susceptibility mapping in Trabzon, NE Turkey. *Catena* 85 (3): 274-287.
87. Yang, X.Q., Kushwaha, S.P.S., Saran, S., Xu, J., and Roy, P.S. 2013. Maxent modeling for predicting the potential distribution of medicinal plant, *Justicia adhatoda* L. in Lesser Himalayan foothills. *Ecol. Eng.* 51: 83-87.
88. Yesilnacar, E.K. 2005. *The Application of Computational Intelligence to Landslide Susceptibility Mapping in Turkey* (PhD Thesis). Department of Geomatics the University of Melbourne, 423p.
89. Yilmaz, I. 2010. The effect of the sampling strategies on the landslide susceptibility mapping by conditional probability (CP) and artificial neural network (ANN). *Environ. Earth Sci.* 60: 505-519.
90. Yost, A.C., Petersen, S.L., Gregg, M., and Miller, R. 2008. Predictive modeling and mapping sage grouse (*Centrocercus urophasianus*) nesting habitat using Maximum Entropy and a long-term dataset from Southern Oregon. *Ecological Informatics*, 3(6): 375-386.
91. Youssef, A.M., Al-Kathery, M., and Pradhan, B. 2014. Landslide susceptibility mapping at AlHasher Area, Jizan (Saudi Arabia) using GIS-based frequency ratio and index of entropy models. *Geosci J.* doi:10.1007/s12303-014-0032-8.
92. Youssef, A.M., Pourghasemi, H.R., Pourtaghi, Z.S., and Al-Katheeri, M.M. 2016. Landslide susceptibility mapping using random forest, boosted regression tree, classification and regression tree, and general linear models and comparison of their performance at Wadi Tayyah Basin, Asir Region, Saudi Arabia. *Landslides* 13 (5): 839-856.
93. Youssef, A.M., Pradhan, B., Jebur, M.N., and El-Harbi, H.M. 2015. Landslide susceptibility mapping using ensemble bivariate and multivariate statistical models in Fayfa area, Saudi Arabia. *Environ. Earth Sci.* 73: 3745-3761.
94. Zhao, C., Chen, W., Wang, Q., Wu, Y., and Yang, B. 2015. A comparative study of statistical index and certainty factor models in landslide susceptibility mapping: a case study for the Shangzhou District, Shaanxi Province, China. *Arab. J. Geosci.* 8 (11): 1-10.
95. Zhao, Y., Huang, Y., Liu, H., Wei, Y., Lin, Q., and Lu, Y. 2018. Use of the normalized difference road landside index (NDRLI)-based method for the quick delineation of road-induced landslides. *Sci. Rep.* 8 (1): 17815.
96. Zipkin, E.F., Grant, E.H.C., and Fagan, W.F. 2012. Evaluating the predictive abilities of community occupancy models using AUC while accounting for imperfect detection. *Ecological Applications*, 22(7): 1962-1972.